

End-to-end RNA Secondary Structure Prediction using Deep Neural Network

1 Introduction

Unlike DNA which typically forms stable double helix between two molecules, RNA is highly flexible such that a single RNA molecule can fold onto itself by forming base pairs via hydrogen bonds, including Watson-Crick pairs A-U, G-C and non-canonical pairs such as G-U. Base pairs form local structures like stems and loops, which assemble into the global secondary structure.

State-of-the-art RNA secondary structure prediction algorithms, such as ViennaRNA[1] and Mfold[2], are based thermodynamics. Each type of local structure comes with free energy that is measured experimentally, and total free energy is assumed to be the sum of all local free energy, which is minimized efficiently using dynamic programming. Although researchers have worked out a large set of local structure types and their associated formulation for free energy calculation, there is no guarantee that it's either accurate or complete. There has been effort to fine tune the free energy parameters by training on experimentally solved structures[3], but it's still limited by the known set of local structure types. Another limitation of dynamic programming based approaches is that it is incapable of predicting nested base pairs that appear in structure like pseudoknot.

Moreover, over the last decade, combination of RNA structure probing and high throughput sequencing has enabled the measurement of genome-wide RNA structural at single nucleotide resolution in multiple organisms and cell types (TODO citation). Due to the level of noise and missing data present in high throughput experiments, we will need a modelling approach that is more flexible and can be trained on different types of data.

In this work, we propose a deep neural network that can be trained end-to-end on sequences and structures. When conditioned on the input RNA sequence, the model can generate a distribution of structures, including ones with pseudoknot.

1.1 Problem Formulation

Given a RNA sequence of length L , we are interested in all possible secondary structures it can take on. For a specific structure, there are three common ways to represent it: (1) Undirected graph, where each node is a base in the sequence, and each vertex represents base pairing. (2) Upper triangular matrix (excluding the diagonal) of size $L \times L$ with binary values, where a value of 1 at (i, j) represents base pairing between sequence position i and j , and 0 represents no base pairing. (3) Dot-bracket notation of length L where unpaired bases are denoted as dots, and paired bases are represented as left and right brackets. When pseudoknot is present, different styles of bracket needs to be used to represent nested structures.

As an example, for a short RNA sequence GUUGU-

GAAU, one possible structure it can take on consists of a stem and a loop, as seen in Fig 1(a), represented by an undirected graph. Such structure can also be represented by an upper triangular 10×10 matrix with all 0's, except for positions (1, 10), (2, 9) and (3, 8), all being 1, as shown in Fig 1(b). This contiguous stretch of 1's along the diagonal corresponds to the stem formed by the three base pairs: G-U, U-A and U-A. The equivalent dot-bracket notation is shown in Fig 1(c), where the three pairs of left-right brackets represent the stem.

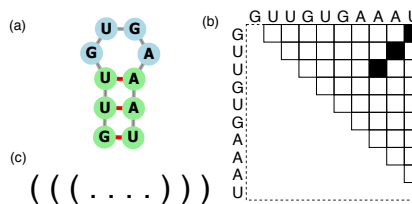


Figure 1: Three different ways to represent secondary structure. (a) undirected graph, generated by [5], (b) upper triangular binary matrix, (c) dot-bracket notation.

1.2 Related Work

Several groups have tried to apply neural network in modeling RNA secondary structure. To the best of our knowledge, existing work either solves a partial problem, or attempts at modelling the problem end-to-end, but requires complicated post-processing to yield valid structure prediction.

Wu[6] presented a convolution neural network to predict the free energy of local structure motifs. Convolution was run on circular matrix representation of the structure motif, to reflect the loop-like nature of local structures. Although it shows promising result on modeling free energy of short structure motif from experimental data, and can be used to estimate the free energy for a *given* structure, it does not solve the problem of predicting structure from sequence.

Other work were done to tackle the learning problem end-to-end. Researchers have framed the problem as a sequence to sequence learning task, and the proposed model either predicts the probability of being paired for each base, or some forms of the dot-bracket notation. Willmott et. al[7] proposed a bidirectional LSTM that predicts from RNA sequence the probability for 3 classes: paired, unpaired, and end-of-Sequence. The model was trained on experimentally solved structure of 16S rRNAs. It is unclear whether the model generalize to other types of RNAs. Zhang et. al[8] proposed using convolutional neural network to predict from sequence the dot-bracket notation, where each position is encoded as a 3-class softmax: left bracket, right bracket and dot. In order for a dot-bracket notation to yield valid structure, it has to follow a few syntactic constraints. For example, each left bracket needs to have a corresponding right bracket. As the authors have mentioned in the paper, output produces by the neural network is not guaranteed to be valid, thus needs to be further processed by dynamic programming to yield a valid structure prediction. Wang et. al[9] used bidirectional LSTM and modelled the dot-bracket notation as a 7-class softmax, which also includes additional bracket notations to allow for pseudoknots. Similar to [8], the prediction does not yield a valid structure, and needs to be corrected by additional logic. Furthermore, they used a dataset of only four RNA families, but reported performance based on randomized training and validation set split. Random split is almost certain to result in sequences from the same family to be in both the training and validation set, thus the generalization performance of the model remains unclear.

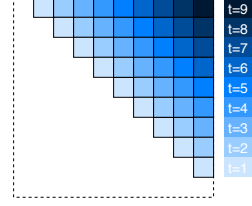


Figure 2: Generative process implied by Equation 1.

2 Method

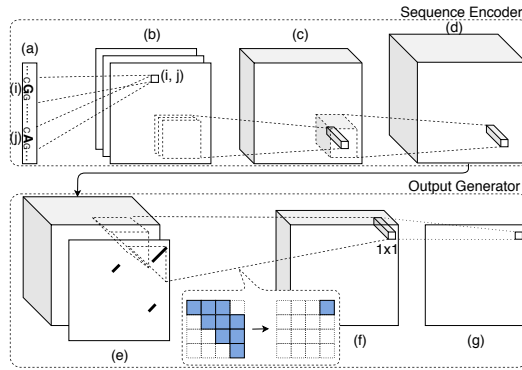


Figure 3: Proposed model architecture. Top: sequence encoding. Bottom: generate structure.

In this work, we propose a deep neural network that can be trained end-to-end on dataset with sequences and structures. The model is capable of generating a distribution of structures conditioned on the input sequence, including structures with pseudoknot.

We formulate the predictive task as a conditional generative process. Specifically, given an input sequence with arbitrary length L : $\mathbf{x} = x_1, x_2, \dots, x_L$, we want to predict a distribution of structures conditioned on the sequence $P(\mathbf{Y} | \mathbf{x})$, where the structure \mathbf{Y} is represented by an upper triangular matrix of size $L \times L$, as defined in Fig 1(b).

We factorize the conditional distribution as follows:

$$P(\mathbf{Y} | \mathbf{x}) = P(\{y_{i,i+1}\}_{i=1,2,\dots,L-1} | \mathbf{x}) P(\{y_{i,i+2}\}_{i=1,2,\dots,L-2} | \mathbf{x}, \{y_{i,i+1}\}_{i=1,2,\dots,L-1}) \dots P(y_{1,L} | \mathbf{x}, \{y_{i,j}\}_{j \neq 1}^{i \neq 1}) \quad (1)$$

The generative process implied by such formulation is illustrated in Fig 2. We generate one off diagonal slice at a time, conditioned on the input sequence and the previous slices, starting from the one adjacent to the diagonal line, shown in light blue with $t = 1$. This process continues until we fill the upper triangular matrix, where the last entry (dark blue, with $t = 9$) is generated conditioned

on the input and the entire upper triangular matrix except for itself. Intuitively, the distance to the off-diagonal line is the "timestamp" as in traditional autoregressive models.

2.1 Model

We propose an architecture that builds global structure from local interactions between all positions on the sequence, without having any assumptions on the types of local structure and without hard-coded parameters, such that the entire model can be trained end-to-end using only sequences and structures. The architecture consists of the following components:

- Two sets of 1D convolution layers on the one-hot-encoded sequence are run in parallel, each set has multiple convolution layers at different resolutions. Activations of the 1D conv layer, one from each set, are used to form a 2D feature map via inner product along the feature dimension, as shown in Fig ?? from (a) to (b). This is inspired by the fact that base pairing is not only affected by the two bases but also surrounding sequences. Such architecture enables the neural network to learn features that affect interaction between any two positions in the sequence. (TODO number of layers, filter size)
- Multiple 2D feature maps, each being the inner product of 1D activations at a specific layer, are concatenated (Fig ?? (b) to (c)), followed by a several 2D conv layers (Fig ?? (c) to (d)).
- Activation of the last 2D conv layer is concatenated with target from the previous "timestamp" y^{t-1} , and the output is generated by an upper triangular convolution, as shown in Fig 3 from (e) to (f), which masks "future" timestamps and ensure the output is generated in auto-regressive fashion.
- Finally, there is a fully connected layer along the feature dimension, with sigmoid activation to produce an output between 0 and 1, for each position in the upper triangular matrix, as illustrated in Fig ?? (f) to (e).

2.2 Training

We trained the model using a synthetic dataset, constructed by sampling 50000 random sequences with length between 10 and 100. For each sequence, we ran RNAfold[1] with the default parameters and record the minimum free energy structure.

For each minibatch, we zero-pad the sequence array and structure matrix to the maximum length in the minibatch. When computing the loss and gradient, entries in structure matrix that were padded are being masked, in addition to the lower triangular entries, since we're only predicting the upper triangular matrix. At training time, prediction, loss and gradient of all positions in the output can be computed in parallel, by passing in the target structure matrix as both the input and target.

2.3 Inference

At test time, we can sample structures conditioned on the input sequence. As shown in Fig 4, we initialize the output structure with a matrix of all zeros, then sample one slice at a time until the upper triangular matrix is filled with sampled values. At each step, we sample a binary label for each position in the current slice based on the Bernoulli probability predicted by the model. To ensure the sampled structure is valid, when sampling the label for location (i, j), if i-th or j-th position is already paired with another position (from samples in the previous timestamps), then we set $y_{i,j}$ to 0 without sampling from the model output. For a sequence of length L , we need to run $L - 1$ steps sequentially. Note that multiple outputs can be sampled in parallel at test time.

3 Result

3.1 Test set performance

We generated a test set with 100 sequence, using a process similar to the training set. Sequences are generated uniformly randomly using A,C,G,U and lengths are between 10 and 100. For each sequence in the test set, we ran RNAfold (TODO more details) and sampled 100 structures from the ensemble, and used our model to also sample 100 from the output distribution conditioned on

the input sequence. To avoid evaluating on low probability structures, we discarded structures that only occur once. Then, for each unique structure produced by RNAfold, we computed sensitivity (TODO definition) and positive predictive value (PPV, TODO definition) against all unique structures generated by our model, and recorded the best one, where best is defined by largest ? (TODO update code + plot, since we're not using f-measure, maybe do a sum?). This represent? how well the model recovers each of structures produced by RNAfold. Histogram showing the distribution of these performance metric across all structures in all sequences is shown in Figure ?? . As we can see from the figure, majority of the RNAfold-generated structures can be recovered with larger than 0.8 sensitivity and PPV.

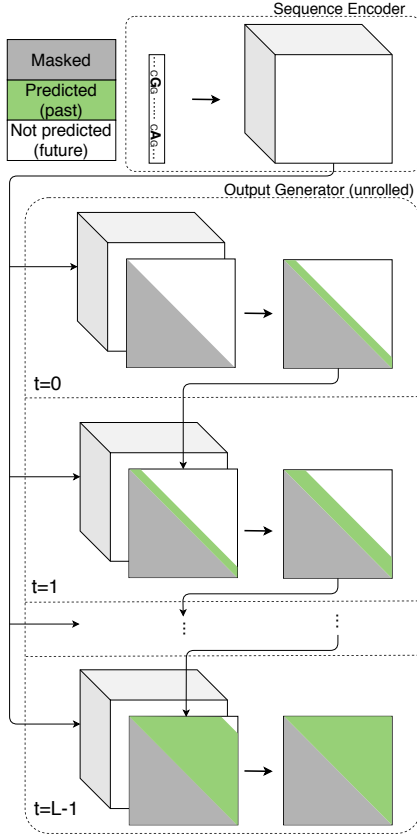


Figure 4: Sample structures conditioned on the input sequence.

3.2 Structure with pseudoknot

Although trained on synthetic dataset with no pseudoknot structures, since our model doesn't incorporate hard-wired rules on how local structures assemble into global structure, it is actually capable of generating structure with pseudoknots. As an example, we use the sequence of mouse mammary tumor virus (MMTV), whose secondary structure contains pseudoknot as measure by nuclear magnetic resonance (NMR), as shown in Fig 6(a). Minimum free energy structure predicted by RNAfold takes a quite different form, which is shown in Fig 6(b). In contrast, when we sample 100 structures from our model, it shows a diverse set of possible structures, including the one predicted by RNAfold, as shown in Fig 6(c3), and more interestingly, the pseudoknot structure from NMR, as shown in Fig 6(c1).

3.3 Sequence design via gradient ascent

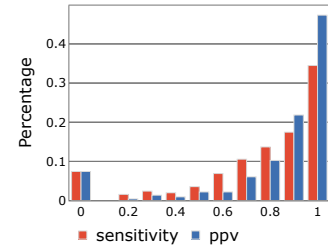


Figure 5: TODO

One benefit of having a differentiable model like neural network is that we can answer interesting questions like: given my current input sequence, what (small) changes can I make to maximize the pairing probability of two positions? We illustrate this using a short RNA sequence GAUCACCUUUGGAUC. (TODO mention sampled structures), with structure as shown in Fig ??(a). In order to find small, local changes to be made on this sequence, we computed the gradient of one output node $y_{i,j}$ with respect to all the input nodes (17×4 array). We ran 100 gradient ascent iterations with step size 0.01, in each step, after adding the gradient (times step size) onto the input, we re-normalize the input so the feature dimension sum up to 1. Fig ??(b) and (c) shows the resulting sequence and structure for $y_{5,11}$ and $y_{6,10}$, respectively.

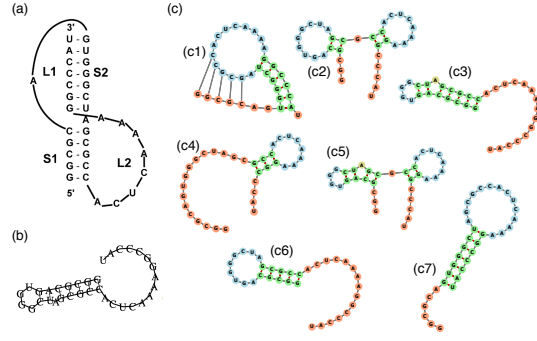


Figure 6: Secondary structure of mouse mammary tumor virus (MMTV): (a) measured by nuclear magnetic resonance (NMR), plot from [10] (TODO plot was a screenshot from the paper, any problems?), (b) predicted by RNAfold web server, (c) Structures generated by our model, specifically, (c1) is a structure with pseudoknot and is identical to (a), (c3) is identical to (b).

4 Conclusion

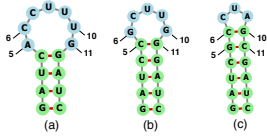


Figure 7: TODO

References

- [1] Ronny Lorenz, Stephan H Bernhart, Christian Höner Zu Siederdisen, Hakim Tafer, Christoph Flamm, Peter F Stadler, and Ivo L Hofacker. Viennarna package 2.0. *Algorithms for molecular biology*, 6(1):26, 2011.
- [2] Michael Zuker. Mfold web server for nucleic acid folding and hybridization prediction. *Nucleic acids research*, 31(13):3406–3415, 2003.
- [3] Mirela Andronescu, Anne Condon, Holger H Hoos, David H Mathews, and Kevin P Murphy. Efficient parameter estimation for rna secondary structure prediction. *Bioinformatics*, 23(13):i19–i28, 2007.
- [4] Mirela Andronescu, Vera Bereg, Holger H Hoos, and Anne Condon. Rna strand: the rna secondary structure and statistical analysis database. *BMC bioinformatics*, 9(1):340, 2008.
- [5] Peter Kerpedjiev, Stefan Hammer, and Ivo L Hofacker. Forna (force-directed rna): simple and effective online rna secondary structure diagrams. *Bioinformatics*, 31(20):3377–3379, 2015.
- [6] Michelle J Wu. Convolutional models of rna energetics. *bioRxiv*, page 470740, 2018.
- [7] Devin Willmott, David Murrugarra, and Qiang Ye. State inference of rna secondary structures with deep recurrent neural networks.
- [8] Hao Zhang, Chunhe Zhang, Zhi Li, Cong Li, Xu Wei, Borui Zhang, and Yuanning Liu. A new method of rna secondary structure prediction based on convolutional neural network and dynamic programming. *Frontiers in genetics*, 10, 2019.
- [9] Linyu Wang, Yuanning Liu, Xiaodan Zhong, Haiming Liu, Chao Lu, Cong Li, and Hao Zhang. Dmfold: A novel method to predict rna secondary structure with pseudoknots based on deep learning and improved base pair maximization principle. *Frontiers in genetics*, 10:143, 2019.
- [10] David W Staple and Samuel E Butcher. Pseudoknots: Rna structures with diverse functions. *PLoS biology*, 3(6):e213, 2005.